

APPLICATION OF THE GIBBS EQUILIBRIUM CONDITIONS TO THE QGP-HADRON TRANSITION CURVE

A. S. Kapoyannis

Department of Physics, University of Athens, 15771 Athens, Greece

Abstract

A method is developed to consistently satisfy the Gibbs equilibrium conditions between the quark-gluon and hadronic phase, although each phase has been formulated in separate grand canonical partition functions containing three quark flavours. The sector in the space of thermodynamic variables, where the transition takes place, is restricted to a curve, according to the phase diagram of QCD. The conservation laws of quantum numbers are also imposed on the transition curve. The effect of the inclusion of the newly discovered pentaquark states is considered. The freeze-out conditions of $S + S$, $S + Ag$ (SPS) and $Au + Au$ (RHIC) are found compatible with a primordial QGP phase, but the conditions indicated by $Pb + Pb$ (SPS) are not.

PACS numbers: 12.40.Ee, 05.70.Fh, 12.38.Mh, 24.10.Pa

Keywords: critical line, QGP-hadron transition, partial chemical equilibrium fugacities, Gibbs equilibrium, heavy-ion

e-mail address: akapog@phys.uoa.gr (A.S. Kapoyannis)

1. Introduction

Quantum Chromodynamics is universally accepted as the theory of strong interactions. Within the context of this theory the phase of Quark-Gluon plasma receives accurate description. However, the formation of the hadronic phase, which is the final state of any possible primordial QGP state, still remains an open problem in view of QCD. On the other hand, the hadronic multiplicities emerging from heavy-ion collisions have been extensively and successfully predicted by statistical models using a handful of thermodynamical parameters [1-8]. So the use of two separate models for the QGP and the hadron phase, called Hadron Gas (HG), offers a complementary approach.

QCD predicts that the transition between QGP and the hadronic phase is a first order one at high baryon densities (depicted by a critical line on the (T, μ_B) plane), while it is of a higher order at small or zero baryon densities (crossover). The end point of the first order transition line is a critical point [9]. The transition points must be restricted to a curve on the phase diagram of temperature and baryon chemical potential. In view of this aspect any models to be used for the description of QGP and HG have to be matched properly at the transition between the two phases.

The aim of this work is to trace the sector of the space of thermodynamic variables, where the QGP-hadron transition occurs, with the following requirements: a) Any mixed phase formed in the first order part of the transition must occupy only a curve in the space of the thermodynamic variables. This requirement is even stronger in the crossover area where a mixed phase does not exist. b) The Gibbs equilibrium conditions have to be satisfied, which amount to $T_{QGP} = T_{HG}$ for thermal equilibrium, $P_{QGP} = P_{HG}$ for mechanical equilibrium and $\{\mu\}_{QGP} = \{\mu\}_{HG}$ for chemical equilibrium, where $\{\mu\}$ stands for the set of chemical potentials used in the description of the two phases. c) All the conservation laws of quantum numbers like baryon number B , electric charge Q , strangeness S , etc. have to be satisfied at every point on the transition line, in a way that they could be extended for every number of flavours that are present in the system.

These problems are confronted every time separate partition functions are used for the two phases, but the simultaneous fulfilment of the above conditions has not been achieved. Among the numerous examples that exist, in [10], where only light, identical quarks are used ($u = d \equiv q$), the curves of equal pressures are made to approximately coincide by a choice on the external parameters B and a_s , something which does not allow matching when other flavours are introduced. In [11] the strange fugacity λ_s is discontinuous at the HG-QGP

transition and the conservation of baryon number can only be accommodated in the case of first order transition. In [12] the strange chemical potential μ_s is also discontinuous. In [13] only q quarks are considered and the requirement of continuity of chemical potentials and conservation of the baryon number leads to a mixed phase which occupies a surface and not a line on the (T, μ_B) plane. The same is true in [14-16] where also s quarks are included. In [17] there is an analogous situation as in [13] with a critical line at the (T, μ_B) plane but the conservation of baryon number is not considered. In [18] the q and s quark chemical potentials are continuous but baryon number and strangeness of the system are not kept constant during hadronisation, since hadrons evaporate from QGP. The considerations of [11-18] are consistent with a first order transition but cannot be valid at the crossover region. In this work all the thermodynamic variables and the pressure will be kept continuous at the transition line (in contrast with [10-12]), the first order part of the transition will be presented by a line on the (T, μ_B) plane (differing from [13-16]), in the mixed phase the quantum numbers will be conserved to each constituent phase (differing from [14]) and no evaporation of hadrons will be assumed from the system (differing from [18]).

Let us consider the requirements that a system with N_f quark flavours has to satisfy. Every conservation law accounts for two equations to be fulfilled. One sets the value of the quantum quantity, e.g. $\langle B \rangle_{QGP} = b_i$ and the other assures the conservation at the phase transition, e.g. $\langle B \rangle_{QGP} = \langle B \rangle_{HG}$. The total number of equations that must hold are, thus, $2N_f + 1$ (the unit accounts for the equality of pressures). Assuming the existence of full chemical equilibrium, every quark flavour introduces one extra fugacity in the set of the thermodynamical variables, which, with the inclusion of volume and temperature, amount to $N_f + 2$. At the crossover region, the surviving free parameters required to fulfil the necessary equations decrease to $N_f + 1$, because of the equality of densities and consequently the equality of volumes between the two phases ($V_{QGP} = V_{HG}$). At the first order transition line the free parameters are $N_f + 2$, since now $V_{QGP} \neq V_{HG}$. It is evident then that the necessary $2N_f + 1$ conditions can be fulfilled only at the first-order part of the transition and only when there is one flavour present, $N_f = 1$, or when the u and d quarks are considered identical (q quarks, described by a single chemical potential μ_q). It has to be clarified that the conditions like $\langle B \rangle_{QGP} = b_i$ have to be satisfied in order to have a whole line of transition points. If these equations are dropped, then we are left with $N_f + 1$ equations, which can be solved, but result to a unique point in the space of the thermodynamical parameters.

2. Expanding the fugacity sector

It is clear that in order to satisfy $2N_f + 1$ relations, every flavour has to be accompanied by two fugacities instead of one. The multiplicity data emerging from heavy ion collisions suggest that the thermalised hadronic system has not achieved full chemical equilibrium. First the strangeness partial chemical equilibrium factor γ_s had been introduced [2] and used extensively to model the data [3-4]. Also a similar factor for the light quarks γ_q was introduced [5] and used in certain analyses [6]. Here the light u and d quarks will be accompanied by separate fugacities γ_u, γ_d . A factor γ_j controls the quark density $n_j + n_{\bar{j}}$ in contrast with the usual fugacity λ_j which controls the net quark density $n_j - n_{\bar{j}}$ [3]. These additional fugacities can serve the purpose of satisfying the necessary equations at the transition point, as well as, preserving the continuity of chemical potentials between the two phases.

A system with 3 flavours (u, d and s quarks) is described by the set of thermodynamical variables $(T, \lambda_u, \gamma_u, \lambda_d, \gamma_d, \lambda_s, \gamma_s) \equiv (T, \{\lambda, \gamma\})$. Setting $x = V_{HG}/V_{QGP}$, the set of equations to be satisfied at every phase transition point will be

$$P_{QGP}(T, \{\lambda, \gamma\}) = P_{HG}(T, \{\lambda, \gamma\}) \quad (1)$$

$$n_{BQGP}(T, \{\lambda, \gamma\}) = x n_{BHG}(T, \{\lambda, \gamma\}) \quad (2)$$

$$n_{QQGP}(T, \{\lambda, \gamma\}) = x n_{QHG}(T, \{\lambda, \gamma\}) \quad (3)$$

$$n_{SQGP}(T, \{\lambda, \gamma\}) = x n_{SHG}(T, \{\lambda, \gamma\}) \quad (4)$$

$$n_{BQGP}(T, \{\lambda, \gamma\}) = 2\beta n_{QQGP}(T, \{\lambda, \gamma\}) \quad (5)$$

$$n_{SQGP}(T, \{\lambda, \gamma\}) = 0, \quad (6)$$

where n denotes densities. For isospin symmetric systems one has to set $\beta = 1$ in (5). Eqs. (1)-(6) only have one free variable, necessary to produce a whole transition line in the phase diagram. At crossover $x = 1$, whereas at the first order transition line the inequality $V_{QGP} \neq V_{HG}$ preserves the survival of x as an extra variable.

3. A solution for the transition curve

The above considerations are applicable to every partition function connected to the hadronic and the quark state. It is interesting, though, to check whether they can produce a real solution for the transition curve, i.e. that the system of equations (1)-(6) is not impossible. For this reason two simple models, will be employed. For the Hadron Gas phase

only the repulsive part of the hadronic interaction will be taken into account through a Van der Waals treatment of the system volume. Also the correct Bose-Einstein or Fermi-Dirac statistics applicable to each hadron will be considered. The hadronic partition function will be extended to all hadronic states containing u , d and s quarks as they are listed in [19]. First, the HG partition function for point particles can be written down as

$$\ln Z_{HG\ pt}(V, T, \{\lambda, \gamma\}) = \frac{V}{6\pi^2 T} \sum_a \sum_i g_{ai} \int_0^\infty \frac{p^4}{\sqrt{p^2 + m_{ai}^2}} \frac{1}{e^{\sqrt{p^2 + m_{ai}^2}/T} \lambda_a^{-1} + \alpha} dp, \quad (7)$$

where g_{ai} are degeneracy factors due to spin and isospin and $\alpha = -1(1)$ for bosons (fermions). Index a runs over all hadronic families, each of which contains members with the same quark content and i over all the particles of this family. The fugacity $\lambda_a = \prod_j \lambda_j^{N_j - N_{\bar{j}}} \gamma_j^{N_j + N_{\bar{j}}}$, where $j = u, d, s$ and $N_j(N_{\bar{j}})$ is the number of $j(\bar{j})$ quarks contained in a hadron belonging to family a . For the light unflavoured mesons with quark content $(c_1/2)(u\bar{u} + d\bar{d}) + c_2 s\bar{s}$, $c_1 + c_2 = 1$, the fugacity used is $\lambda_a = (\gamma_u \gamma_d)^{c_1} \gamma_s^{2c_2}$.

If each hadron i is assumed to occupy volume V_i , then the available volume for the system is reduced to $\Delta = V - \sum_i N_i V_i$, where N_i is the number of particles i present in the system. Assuming that each hadrons' volume is proportional to its mass, then $V_i/m_i = V_0$, with V_0 remaining an open parameter controlling the hadron size. The available volume can be written as $\Delta = V - \sum_i N_i m_i V_0$. Dividing by Δ we get

$$1 = \frac{V}{\Delta} - \rho_{pt} V_0 \Rightarrow \Delta = \frac{V}{1 + \rho_{pt} V_0},$$

where ρ_{pt} is the mass density of a system of point particles at volume Δ . Defining the quantity $f \equiv \rho_{pt} V_0$, it can be calculated to be

$$f = \frac{V_0}{6\pi^2 T} \sum_a \sum_i g_{ai} m_{ai} \int_0^\infty \frac{p^4}{\sqrt{p^2 + m_{ai}^2}} \frac{1}{e^{\sqrt{p^2 + m_{ai}^2}/T} \lambda_a^{-1} + \alpha} dp, \quad (8)$$

where the sum over all particles is organised first to a sum over all families. The available volume is then

$$\Delta = \frac{V}{1 + f}. \quad (9)$$

The partition of the extended hadrons at volume V may be considered equal to the partition function of the point particles at volume Δ

$$\ln Z(V, T, \{\lambda, \gamma\}) = \ln Z_{pt}(\Delta, T, \{\lambda, \gamma\}). \quad (10)$$

The pressure is

$$P_{HG} = \frac{\partial \ln Z_{HG}(V, \dots)}{\partial V} = \frac{\partial \ln Z_{HG\ pt}(\Delta, \dots)}{\partial V},$$

or by using eq. (9)

$$P_{HG} = \frac{P_{HG\ pt}}{1+f} . \quad (11)$$

In a similar manner the densities are calculated to be

$$n_{i\ HG} = \frac{n_{i\ HG\ pt}}{1+f} \quad (12)$$

For the QGP phase a simple model containing 3 flavours is used. The quarks are non-interacting and only the presence of gluons is accounted for, as well as the effect of the vacuum through the MIT bag constant, B . A wealth of quark fugacities is easily accommodated, though, in this model. The QGP partition function is consequently

$$\ln Z_{QGP}(V, T, \{\lambda, \gamma\}) = \frac{N_s N_c V}{6\pi^2 T} \sum_j \int_0^\infty \frac{p^4}{\sqrt{p^2 + m_j^2}} \frac{1}{e^{\sqrt{p^2 + m_j^2}/T} (\lambda_j \gamma_j)^{-1} + 1} dp + V \frac{8\pi^2 T^3}{45} - \frac{BV}{T} , \quad (13)$$

where $N_s = 2$ and $N_c = 3$. Index j runs to all quarks and antiquarks and the fugacity $\lambda_{\bar{j}} = \lambda_j^{-1}$ and $\gamma_{\bar{j}} = \gamma_j$. The current quark masses are $m_u = 1.5$, $m_d = 6.75$ and $m_s = 117.5$ MeV [19].

At the first order QGP-HG transition a mixed phase is assumed. This phase spans over a curve in the $(T, \{\lambda, \gamma\})$ -space, so these variables are kept constant throughout the mixed phase. The only thermodynamic variable which is allowed to change is the system volume V . The volume equals V_{HG} at the pure hadronic phase, at one end of the first order transition and V_{QGP} at the pure quark phase, at the other end of the transition. The partition function of the mixed phase can then be written down as

$$\ln Z_{mixed}(V, T, \{\lambda, \gamma\}) = \delta \ln Z_{HG}(V_{HG}, T, \{\lambda, \gamma\}) + (1 - \delta) \ln Z_{QGP}(V_{QGP}, T, \{\lambda, \gamma\}) . \quad (14)$$

The parameter δ is $0 \leq \delta \leq 1$ and for $\delta = 1$ ($\delta = 0$) we have pure HG(QGP) phase. Since in all cases the volume appears as a multiplicative factor in the partition function, the ratio $g \equiv \frac{\ln Z}{V}$ does not depend on the volume. Then eq. (1) suggests that at every transition point

$$g_{HG}(T, \{\lambda, \gamma\}) = g_{QGP}(T, \{\lambda, \gamma\}) . \quad (15)$$

Then eq. (14) is equivalent to

$$\ln Z_{mixed}(V, T, \{\lambda, \gamma\}) = [\delta V_{HG} + (1 - \delta) V_{QGP}] g_{HG}(T, \{\lambda, \gamma\}) , \quad (16)$$

suggesting that the system volume V of the mixed phase can be defined as

$$V = \delta V_{HG} + (1 - \delta) V_{QGP} . \quad (17)$$

Through eqs. (1), (16) and (17), the pressure in the mixed phase can be calculated for every V to be

$$P_{mixed} = \frac{kT \ln Z_{mixed}(V, T, \{\lambda, \gamma\})}{V} = kT g_{HG}(T, \{\lambda, \gamma\}) = P_{HG} = P_{QGP} . \quad (18)$$

The pressure is, consequently, kept constant throughout the first order transition. The part of the $P-V$ isotherm which corresponds to the mixed phase is parallel to the V axis, as it is expected in a first order transition.

On the contrary, the densities vary. Let λ_i be the fugacity associated with the density n_i . Then

$$n_{i \text{ mixed}} = \frac{1}{V} \lambda_i \frac{\partial \ln Z_{mixed}(V, T, \{\lambda, \gamma\})}{\partial \lambda_i} = \frac{1}{V} \left[\delta V_{HG} \lambda_i \frac{\partial g_{HG}(T, \{\lambda, \gamma\})}{\partial \lambda_i} + (1 - \delta) V_{QGP} \lambda_i \frac{\partial g_{QGP}(T, \{\lambda, \gamma\})}{\partial \lambda_i} \right] ,$$

or

$$n_{i \text{ mixed}} = \frac{\delta V_{HG}}{\delta V_{HG} + (1 - \delta) V_{QGP}} n_{i \text{ HG}} + \frac{(1 - \delta) V_{QGP}}{\delta V_{HG} + (1 - \delta) V_{QGP}} n_{i \text{ QGP}} . \quad (19)$$

It is easily checked that for $\delta = 1$ ($\delta = 0$) the density of the pure hadronic(quark) state is produced. The conservation of the quantum quantities B , Q and S is assured in the mixed phase. Eq. (2) implies that $\langle B \rangle_{HG} = \langle B \rangle_{QGP}$. Then multiplying the two sides of eq. (19) by V gives

$$V n_{B \text{ mixed}} = \delta \langle B \rangle_{HG} + (1 - \delta) \langle B \rangle_{QGP} \Rightarrow \langle B \rangle_{mixed} = \langle B \rangle_{HG} = \langle B \rangle_{QGP} . \quad (20)$$

Eqs. (3)-(4) produce similar equations for Q and S .

Between the crossover region (where $x = 1$) and the first order transition line (where $x \neq 1$) the critical point resides. Observing eqs. (1)-(6) it is clear that they do not provide a restriction on x , other than it should be a continuous function. So these equations can accommodate an additional constraint in the form of x , which may be provided by a sophisticated partition function that records the full part of interaction (attractive part as well).

The system of eqs. (1)-(6) can then be solved for $x = 1$ for the crossover region or for $x \neq 1$ for the first order transition curve. The system is simplified observing that the strangeness neutrality at the QGP phase (eq. (6)) leads to the solution $\lambda_s = 1$. This solution is valid for every case of QGP partition function, as long as products of the fugacities of the strange quark with the fugacities of u or d quarks do not appear. The initial system then is reduced

to the system of eqs. (1)-(5) for $\lambda_s = 1$. The HG partition function (7), (10) and the QGP partition function (13) is used to the system of eqs. (1)-(5). For the particular choices of partition functions, two parameters, B and V_0 , are left open, producing different solutions for the transition curves. The system of eqs. (1)-(5) for $\lambda_s = 1$ accepts as solution for the variable γ_s the value 0, since then eq. (5) is automatically satisfied. This a trivial solution because it is equivalent to the absence of the strange quarks in the system and therefore such solutions should be excluded. Non-trivial solutions for the thermodynamic variables are depicted for the parameters $B^{1/4} = 280$ MeV and $V_0 = 1.4/(4B)$ in Figs. 1-4 for the isospin symmetric case ($\beta = 1$). Lines (a) represent the solution without the inclusion of pentaquarks. The crossover region, which is determined uniquely after setting the parameters B and V_0 , is drawn everywhere with slashed lines.

Two additional matters concerning the phase transition are the position of the critical point where the crossover region ends and the first order transition sets in, as well as, the ratio of the volumes $x = V_{HG}/V_{QGP}$ at the first order transition line. These two matters cannot be dealt with the simple choices of partition functions used for the calculations of this section, since the attractive part of the interaction among hadrons or quarks is completely neglected. To display certain solutions for the critical curve within the context of the partition functions (7), (10) and (13), a position for the critical point has to be chosen. This position is set at $\mu_{B\ cr.p.} = 360$ MeV, according to the result of [20], where the critical point is located by lattice QCD calculations using three quark flavours and considerably reduced light quark masses, approaching their physical values. Eqs. (1)-(6) for $x = 1$ is a system of 6 equations with 7 variables. Adding one more equation ($\mu_{B\ cr.p.} = 360$ MeV) a system with 7 equations is formed, which is solved to determine the full set of thermodynamic variables that correspond to the position of the critical point.

A form for the ratio of the volumes x also has to be defined. This form has to produce $x = 1$ at the position of the critical point. Moreover, it is chosen to produce a given value x_1 at a specific value of $\lambda_{u\ 1}$. A simple form which implements these demands is

$$x = 1 + \left(\frac{\ln \lambda_u - \ln \lambda_{u\ cr.p.}}{\ln \lambda_{u\ 1} - \ln \lambda_{u\ cr.p.}} \right)^\epsilon (x_1 - 1) , \quad (21)$$

where the exponent ϵ regulates the curvature of the first order transition line. For lines (a) $x_1 = 1.1$ at $\lambda_{u\ 1} = 14.2$ and $\epsilon = 1.5$ are chosen. Of course, any function of x can be used, producing different first order transition curves. The resulting first order transition lines are drawn with solid lines in Figs 1-4, while the respective critical points are represented by solid

circles.

Temperature T is displayed as function of the baryon chemical potential μ_B in Fig. 1. In the same figure, line (d), which represents the phase transition line as it is calculated from the Lattice QCD in [21], is drawn for comparison. The relative chemical equilibrium fugacity γ_u is displayed as function of μ_B in Fig. 2. This particular solution leads to the gradual suppression of γ_u as baryon chemical potential increases. The connection of γ_u and γ_d , for isospin symmetric solution, is depicted in Fig. 3. The line $\gamma_u = \gamma_d$ is also drawn for comparison. The relative chemical equilibrium factor γ_s is drawn as a function of the baryon chemical potential in Fig. 4.

In Fig. 5 the ratios of volumes x , which are used in the first order transition, are drawn against the baryon chemical potential. The used forms of x are increasing functions with respect to the baryon chemical potential. The resulting first order transition lines produce smaller temperatures as the baryon chemical potential increases, something which is expected.

One direct consequence of the simultaneous solution of eqs. (1)-(6) is that the relative chemical equilibrium fugacities have values that depend on each other at every transition point. This is easily realised by inspecting the condition $n_{SHG} = 0$ (for $\lambda_s = 1$). The solution of this condition is greatly simplified by the use of the Boltzmann approximation and the assumption that isospin symmetry leads to the approximate solution $\lambda_u = \lambda_d \equiv \lambda_q$ and $\gamma_u = \gamma_d \equiv \gamma_q$. Neglecting trivial solutions, where $\gamma_s = 0$, the zero strangeness condition can be solved to give

$$\gamma_s = \frac{F_K(T) - F_H(T)\gamma_q(\lambda_q + \lambda_q^{-1})}{2F_{\Xi}(T)}. \quad (22)$$

In eq. (22), F_K corresponds to the Kaon mesons, F_H to the Hyperon baryons (Λ 's and Σ 's) and F_{Ξ} to the Ξ baryons, while the summation

$$F_a(T) = \frac{T}{2\pi^2} \sum_i g_{ai} m_{ai}^2 K_2\left(\frac{m_{ai}}{T}\right) \quad (23)$$

to all particles i of the same family is implied. In the above relation, K denotes a modified Bessel function of the second kind. It is evident from eq. (22) that the increase of the relative chemical equilibrium factor for light quarks, γ_q and the increase of the light quark fugacity, λ_q , leads, at constant temperature, to the decrease of factor γ_s .

4. Inclusion of pentaquarks

There has been recent evidence of hadrons containing five quarks. These 5-quark states are the $\Theta^+(1540)$ [22] with $I = 0$ and quark content $uudd\bar{s}$ and the $\Xi^*(1862)$ with $I = 3/2$. The content of the states $\Xi^*(1862)$ is $ssdd\bar{u}$ (for the state with electric charge $Q=-2$), $ssud\bar{u}$ (with $Q=-1$), $ssudd\bar{d}$ (with $Q=0$) and $ssuud\bar{d}$ (with $Q=+1$). The existence of the first three of the states $\Xi^*(1862)$ has been confirmed [23]. The motivation to investigate the effect of the pentaquark states comes from the fact that these states can alter eqs. (1)-(6), since they introduce additional hadronic families, each of which is accompanied by completely different functions between the system fugacities compared to the ones in the already known families. This can be easily realised if the corresponding equation of (22) is written down as

$$\gamma_s = \frac{F_K(T) + F_\Theta(T)\gamma_q^3(\lambda_q^2 + \lambda_q^{-2})(\lambda_q + \lambda_q^{-1}) - F_H(T)\gamma_q(\lambda_q + \lambda_q^{-1})}{2[F_\Xi(T) + F_{\Xi^*}(T)\gamma_q^2]}. \quad (24)$$

The existence of Θ hadron drives γ_s to higher values with a strong dependence on γ_q and λ_q , whereas the inclusion of the Ξ^* states contributes to the decrease of γ_s .

The system of eqs. (1)-(6) is then solved with the inclusion of the $\Theta^+(1540)$ and $\Xi^*(1862)$ states with the same partition functions for the HG and the QGP phase and for the same parameters B , V_0 as in the case without the inclusion of the pentaquarks (lines (a) of the previous section). The resulting curves are lines (b), shown in Figs. 1-4. The adopted form of the ratio of volumes x again produces value $x_1 = 1.1$ at $\lambda_{u1} = 14.2$ (while $\epsilon = 1.5$) and is plotted in Fig. 5.

Lines (a) and (b) record the difference induced in the transition curve by the inclusion of the pentaquarks, if parameters B and V_0 remain the same and x acquires the same value at a given value of λ_u . However, none of these parameters is known and so the difference in the transition curve cannot provide evidence for the existence of pentaquarks. For this reason lines (c) are drawn in Figs. 1-4. These lines represent a solution for the transition curve without the inclusion of the pentaquarks but for a different choice of parameters (B remains the same, $V_0 = 1.29/(4B)$, $x_1 = 1.12$ at $\lambda_{u1} = 14.2$ and $\epsilon = 1.15$). It is evident, now, that lines (b) (with pentaquarks included) and lines (c) (without pentaquarks) almost coincide.

5. Application to heavy-ion data

The fact that the transition territory between the hadronic and the QGP phase is restricted to a line in the space of temperature and chemical potentials produces a direct

connection between the variables after the phase transition and the corresponding ones before: they *must coincide*. This is not the case when the transition territory is allowed to occupy a surface. Then the connection between the thermodynamic variables of the hadronic and the quark phase is broken. The system, as it crosses the transition territory to enter the state of hadrons, loses its “memory” of the plasma state.

In a system where the hadronic state carries the memory of its preceding state, one may use the freeze-out variables as a diagnostic tool for a primordial QGP phase. Assuming that (a) a quark-gluon phase *has* been formed in a collision experiment and (b) the chemical freeze-out occurs right after the transition to the hadronic phase, then the freeze-out thermodynamic variables have to fulfil constraints (1)-(6). If, on the contrary, no quark-gluon state is formed before hadronization, then the restriction on the freeze-out conditions of the system is diminished only to eqs.

$$n_{B_{HG}}(T, \{\lambda, \gamma\}) = 2\beta n_{Q_{HG}}(T, \{\lambda, \gamma\}) \quad (25)$$

$$n_{S_{HG}}(T, \{\lambda, \gamma\}) = 0, \quad (26)$$

a set of constraints which will be referred to from now on as set A.

The thermodynamic variables are extracted through a fit of the experimentally measured particle multiplicities or ratios to a statistical model. Such a technique has been successful. If now the additional constraints (1)-(6) are imposed, the question that arises is whether a successful fit is also produced or the restrictions that these constraints imply are inconsistent with the data.

These ideas will now be used to analyse the freeze-out variables of four heavy-ion experiments. The application of eqs. (1)-(6) require the knowledge of the partition functions for the hadron and the quark phase. The particular functions used in sections 4 and 5 to demonstrate a solution include the arbitrariness in the choice of the parameters B , V_0 and quantity x . Since it is unwanted for the extracted variables to depend on the choice of unknown parameters, it is better to form and apply a subset of constraints which are completely independent from these parameters.

When the system of eqs. (1)-(6) is valid, eqs. (3)-(6) can equivalently be rewritten as

$$n_{B_{HG}}(T, \{\lambda, \gamma\}) = 2\beta n_{Q_{HG}}(T, \{\lambda, \gamma\}) \quad (27)$$

$$n_{B_{QGP}}(T, \{\lambda, \gamma\}) = 2\beta n_{Q_{QGP}}(T, \{\lambda, \gamma\}) \quad (28)$$

$$n_{S_{HG}}(T, \{\lambda, \gamma\}) = 0 , \quad (29)$$

$$n_{S_{QGP}}(T, \{\lambda, \gamma\}) = 0 . \quad (30)$$

Eq. (27) results from eqs. (2), (3) and (5), whereas eq. (30) is due to eqs. (4) and (6). It is easily checked that the common denominator (see eq. (12)), which includes the parameter V_0 , cancels out from both sides of eq. (27). The same is true for eq. (29), while eq. (30) is easily solved to give $\lambda_s = 1$. Eqs. (27)-(30) (referred to as Set B) now form a set of equations that do not depend on the parameters V_0 for the particle size, B (MIT bag constant) nor the ratio x applicable to the first order transition line.

On the contrary, eqs. (1) and (2) are model dependent and contain unknown parameters. However, if the freeze-out parameters are determined, they can be inserted in eq. (2) to determine V_0 (assuming that x is known) and then eq. (1) can be used to determine B . This task serves to show that eqs. (1) and (2) have a real solution and contributes to the overall consistency of the technique.

In the following the freeze out variables for the experiments $S + S$ [24], $S + Ag$ [25] (NA35) at beam energy 200 AGeV, $Pb + Pb$ [26] (NA49) at beam energy 158 AGeV and $Au + Au$ [27] (STAR) at $\sqrt{s_{NN}} = 130$ GeV will be analysed. The data used are listed in Table 1 and they are in all cases full phase space multiplicities, except from the RHIC data which are measured in the midrapidity. The experiments to be analysed are chosen because they do not produce great baryon chemical potential at freeze out and so they are probably at the crossover area [20], allowing one to set $x = 1$. The technique can be applied to the first order transition case, determining the freeze-out variables, since the equations of set B do not depend on x , but then the parameters V_0 and B cannot not be uniquely determined.

The theoretical calculation of the particle multiplicity necessary to perform a fit to the experimental data has been carried out with the partition function (7), (10). The right Bose-Einstein or Fermi-Dirac statistics for every particle has been used throughout the calculations. The feeds from the decay of resonances have also been included. The value of β is set to 1 in the case of $S + S$, 1.1 in the case of $S + Ag$, 1.27 for $Pb + Pb$ and 1.25 for $Au + Au$.

In Tables 2 (a)-(b) the freeze-out variables are extracted with the assumption of no primordial QGP phase (constraints of set A), whereas in Tables 3 (a)-(b) the primordial QGP phase is assumed, thus applying constraints of set B. Another matter concerning the analysis is the observation that the inclusion of the pion multiplicity deteriorates the fit

[8,28]¹. Since the quality of the fitting procedure is of importance in evaluating the results and a bad fit, when the constraints of set B are imposed, may be partly due to the presence of the pion multiplicity, two fits are performed in each case, one with all the multiplicities included (Tables (a)) and one without the multiplicities that contain pions (Tables (b)). This makes clear the effect of the pion multiplicities in the overall procedure. In any case, the fits without the pions are in general more reliable.

The first observation which can be made by comparing the first and the second part of every table is that the inclusion of pentaquarks has negligible effect on the evaluated parameters or the quality of the fit. So one can safely draw equivalent conclusions by performing the analysis with the pentaquarks or without them.

For the $S + S$ and $S + Ag$ data the fit with set B is of medium quality ($\chi^2/dof = 2.95$ and 1.92 , respectively) when the pions are present. This is not far worse, though, than the fit in the case of set A. When the pions are excluded, the fit with set B turns out to be very good ($\chi^2/dof = 0.47$ and 0.065 , respectively), while the temperature remains at acceptable values, proving these cases to be completely compatible with a primordial quark-gluon phase. Another observation is that the imposition of set B with respect to set A, in every case, does not produce a dramatic change in the quality of the fit.

In the case of $Pb + Pb$ the fit is relatively good with the imposition of set A ($\chi^2/dof = 2.50 - 1.79$), but the imposition of set B severely worsens the quality of the fit. The situation cannot be remedied with the exclusion of pions and χ^2/dof remains at the value of $18.0 - 18.2$. The conclusion to be drawn from the bad quality of the fit with the imposition of the constraints of set B, is that the data of this experiment are not compatible with a preceding QGP phase. The dramatic change in the quality of the fit between the cases of set A and B, should be noted as well. Also the freeze-out temperature in case of set B is unrealistically high and rises enormously with respect to the case of set A.

The findings concerning the $S + S$ and $S + Ag$ data are also in agreement with the proximity of the chemical freeze out points of these experiments to the Statistical Bootstrap critical line which was found in [8]. On the contrary, the freeze out point of $Pb + Pb$ was not found to possess such an attribute in [30], which is also in agreement with the present results.

In case of RHIC and in case of set A the value of χ^2/dof is 1.51 , when the pions are

¹The presence of excess of pions, though, can be connected with a primordial high entropy phase or with a phase with the chiral symmetry restored [29].

included and this value diminishes to 0.229, when the pions are excluded. Similar results are obtained when set B is imposed. The fit in the presence of pions is of not so good quality ($\chi^2/dof = 3.86$) and the temperature acquires too high value. The fit turns out to be quite good, though, when the pions are excluded ($\chi^2/dof = 1.19$) and the temperature remains at acceptable values, so the thermodynamic parameters are compatible with a QGP phase.

The extracted parameters in case of set B are inserted to eqs. (1) and (2) and the parameters V_0 and $B^{1/4}$ are also determined. It is interesting that in the cases of $S + S$, $S + Ag$ and $Au + Au$ (without the pions), which have been proven to be compatible with set B, all the calculated values of V_0 and $B^{1/4}$ are close, compatible with a unique value for these parameters. On the contrary, the $Pb + Pb$ case produces values of V_0 and $B^{1/4}$ with no connection with the rest cases.

The necessity of the expansion of the fugacity sector with the partial equilibrium fugacities is also revealed with the application of the present technique. If these fugacities are set to $\gamma_u = \gamma_d = \gamma_s = 1$, then the sector of the phase space which is compatible with the QGP-hadron transition is severely limited. In such a case, if a similar fit to the one with set B is performed, apart from the fact that eqs. (27) and (28) cannot be accommodated, the fit turns out to be worse. The result in the case without the pions is then $\chi^2/dof = 0.617, 1.09, 28.0$ and 1.83 for $S + S$, $S + Ag$, $Pb + Pb$ and $Au + Au$ respectively. Then in the case of $Au + Au$ the compatibility with the QGP phase turns out to be dubious.

Another general observation, which can be drawn from Tables 2-3, is that in the cases which are compatible with a primordial QGP phase ($S + S$, $S + Ag$ and $Au + Au$) the inclusion of the pions in the fits produces a dramatic increase in the χ^2/dof value relative to the fits without the pions. Also the fitted temperature is calculated to be much higher in the presence of pions. This is checked from comparing the value of χ^2/dof and the temperature in Tables (b) and (a). Although in the present work the fugacities γ_u and γ_d are used, which describe off chemical equilibrium effects and the pion content is u and d quarks, this dramatic increase in the χ^2/dof and the temperature when the pions enter the fit, persists. Thus, for the QGP compatible cases, the γ_u and γ_d fugacities cannot improve the fit to acceptable limits and reveal that an excess of pions is present to these cases.

It is evident by incorporating all the previous analyses, that for the $S + S$, $S + Ag$ and $Au + Au$ cases, the freeze-out thermodynamic variables should be considered these of Table 3 (b). For the $Pb + Pb$ case the relevant freeze-out variables should be considered these of Table 2 (a) or 2 (b).

Gathering the observations made in this section, what it found is that the freeze-out conditions of some experiments are compatible with a QGP phase (constraints B). This is revealed from the fact that the imposition of constraints B produces fits with acceptable values of χ^2/dof and temperature. The opposite is true for the experiments incompatible with the QGP phase. In such cases the imposition of constraints B leads to high values χ^2/dof and temperature, though these values are acceptable, when only constraints A (no QGP phase assumed) are imposed. Also, the QGP compatible cases present an excess in the pion multiplicity which cannot properly be fitted (in these cases) by the γ_u and γ_d fugacities. This is seen by a great increase in the value of χ^2/dof and temperature when the pions are included in the fit in comparison to the fits without pions, for both cases of constraints A and B.

6. Conclusions

Although two different partition functions are used for the description of the quark and hadronic side of matter, it is possible to preserve the continuity of all chemical potentials and, of course, temperature and pressure (Gibbs equilibrium conditions) at the transition region, which is confined to a curve. Also, all the constraints imposed by the conservation laws of quantum quantities can be applied, leading, at the same time, to a non-trivial solution of the thermodynamic variables into a three quark flavour system. The key issue for the success of this project is the expansion of the fugacity sector of the available variables and the, already, introduced relative chemical equilibrium variables can be used to serve that purpose.

Despite the fact that the space of the thermodynamic variables is extended, the restrictions imposed on the transition points produce relations among these variables. A part of these relations, in a simple form, is expressed in eq. (22) or (24).

The restrictions on the freeze-out conditions, imposed by the existence of a quark-gluon state in the early stages after a collision experiment, can be applied to every case where the thermalisation of the produced hadrons has been proven. They can serve to separate the experiments compatible with QGP state from those which are not. The expansion of the fugacity sector with the partial equilibrium fugacities, though, magnifies the part of the phase space allowed by such constraints.

The whole methodology which was presented can be used for every grand canonical partition function adopted for the description of the HG or QGP phase. The inclusion of interaction is crucial for the prediction of the critical point and the volume expansion ratio,

which could not be determined by the models used in this work. At the moment, lattice calculations have led to the determination of the accurate quark-gluon equation of state with three quark flavours at finite baryon chemical potential [20,31]. It would be interesting, though, if these calculations could be extended with the inclusion of the relative chemical equilibrium variables for light and strange quarks, allowing for matching with the existing hadron gas models. For the hadronic side of matter the inclusion of the attractive part of interaction can be incorporated via the statistical bootstrap [7,8], where the prediction of a critical point is also possible [32]. The incorporation of the full set of parameters γ_i to these studies would allow for a more precise matching with a primordial quark phase.

Acknowledgement I would like to thank N. G. Antoniou, C. N. Ktorides and F. K. Diakonos for fruitful discussions.

References

- [1] J. Cleymans, H. Satz, Z. Phys. C **57**, 135 (1993).
- [2] J. Rafelski, Phys. Lett. B **262**, 333 (1991); J. Letessier, A. Tounsi, J. Rafelski, Phys. Lett. B **292**, 417 (1992).
- [3] C. Slotta, J. Sollfrank, U. Heinz, hep-ph/9504225.
- [4] J. Sollfrank, M. Gaździcki, U. Heinz, J. Rafelski, Z. Phys. C **61**, 659 (1994); M.N. Asprouli, A.D. Panagiotou, Phys. Rev. C **51**, 1444 (1995); J. Letessier, A. Tounsi, U. Heinz, J. Sollfrank, J. Rafelski, Phys. Rev. D **51**, 3408 (1995); F. Becattini, M. Gaździcki, J. Sollfrank, Eur. Phys. J. C **5**, 143 (1998).
- [5] J. Rafelski, J. Letessier, Presented at 15th Winter Workshop on Nuclear Dynamics, Park City, UT, 9-16 Jan 1999, hep-ph/9902365.
- [6] F. Becattini, M. Gaździcki, A. Keränen, J. Manninen, R. Stock, Phys. Rev. C **69**, 024905 (2004); J. Letessier, G. Torrieri, S. Steinke, J. Rafelski, Phys. Rev. C **68**, 061901 (2003).
- [7] R. Hagedorn, Nuovo Cimento Suppl. **III**, 147 (1965); R. Hagedorn, Nuovo Cimento Suppl. **VI**, 311 (1968).

- [8] A.S. Kapoyannis, C.N. Ktorides, A.D. Panagiotou, Phys. Rev. C **58** (1998) 2879; Eur. Phys. J. C **14**, 299 (2000).
- [9] F. Wilczek, hep-ph/0003183; J. Berges, K. Rajagopal, Nucl. Phys. B **538**, 215 (1999); M.A. Halasz, A.D. Jackson, R.E. Shrock, M.A. Stephanov, J.J. Verbaarschot, Phys. Rev. D **58**, 096007 (1998).
- [10] J. Letessier, A. Tounsi Nuovo Cimento A **99**, 521 (1988).
- [11] K. Redlich, Z. Phys. C **27**, 633 (1985).
- [12] K.S. Lee, M.J. Rodes-Brown, U. Heinz, Phys. Lett. B **174**, 123 (1986).
- [13] P.R. Subramanian, H. Stöcher, W. Greiner, Phys. Lett. B **173**, 468 (1986).
- [14] C. Greiner, P. Koch, H. Stöcher, Phys. Rev. Lett. **58**, 1825 (1987).
- [15] B. Lukács, J. Zimányi, N.L. Balazs, Phys. Lett. B **183**, 27 (1987).
- [16] J. Cleymans, M.I. Gorenstein, J. Stalnacke, E. Suhonen, Phys. Scrip. **48**, 277 (1993).
- [17] U. Heinz, P.R. Subramanian, H. Stöcher, W. Greiner, J. Phys. G **12**, 1237 (1986).
- [18] C. Greiner, H. Stöcher, Phys. Rev. D **44**, 3517 (1991).
- [19] K. Hagiwara, et. al., Particle Data Group, Phys. Rev. D **66** No. 1 (2002).
- [20] Z. Fodor, S.D. Katz, JHEP **0404**, 050 (2004).
- [21] Z. Fodor, S.D. Katz, JHEP **0203**, 014 (2002); Z. Fodor, S.D. Katz, talk given at Finite Density QCD at Nara, Nara, Japan, 10-12 July 2003, Prog. Theor. Phys. Suppl. **153**, 86 (2004).
- [22] T. Nakano, et. al., LEPS Collaboration, Phys. Rev. Lett. **91**, 012002 (2003); V.V. Barmin, et. al., DIANA Collaboration, Phys. Atom. Nucl. **66**, 1715 (2003), Yad. Fiz. **66**, 1763 (2003); S. Stepanyan, et. al., CLAS Collaboration, Phys. Rev. Lett. **91**, 252001 (2003); J. Barth, et. al., SAPHIR Collaboration, hep-ex/0307083.
- [23] C. Alt, et. al., NA49 Collaboration, Phys. Rev. Lett. **92**, 042003 (2004); R. Jaffe, talk given at Quark Matter 2004, Oakland, California, January 11 - 17, 2004.

- [24] J. Bartke, et al, NA35 Coll., Z. Phys. C **48**, 191 (1990); J. Baechler, et al., NA35 Coll., Nucl. Phys. A **525**, 59c (1991); J. Baechler, et al., NA35 Coll., Nucl. Phys. A **525**, 221c (1991); J. Baechler, et al., NA35 Coll., Nucl. Phys. A **544**, 293c (1992); J. Baechler, et al., NA35 Coll., Z. Phys. C **58**, 367 (1993); T. Alber, et al., NA35 Coll., preprint IKF-HENPG/6-94; J. Bächler, et al., NA35 Coll., Phys. Rev. Lett. **72**, 1419 (1994); T. Alber, et al., NA35 Coll., Z. Phys. C **64**, 195 (1994); M. Gaździcki, et al., NA35 Coll., Nucl. Phys. A **566**, 503c (1994); T. Alber, et al., NA35 Coll., Phys. Lett. B **366**, 56 (1996).
- [25] J. Baechler, et al., NA35 Coll., Eur. Phys. J. C **2**, 643 (1998); J. Baechler, et al., NA35 Coll., Phys. Rev. Lett. **72**, 1419 (1994); T. Alber, et al., NA35 Coll., Z. Phys. C **64**, 195 (1994); T. Alber, et al., NA35 Coll., Phys. Lett. B **366**, 56 (1996); D. Rohrich, et al., NA35 Coll., Nucl. Phys. A **566**, 35c (1994); F. Becattini, J. Phys. G **23**, 1933 (1997); F. Becattini, M. Gaździcki J. Sollfrank, Eur. Phys. J. C **5**, 143 (1998).
- [26] S.V. Afanasiev, et al., NA49 Coll., Phys. Rev. C **66**, 054902 (2002); S.V. Afanasiev, et al., Nucl. Phys. A **715**, 161 (2003); S.V. Afanasiev, et al., Nucl. Phys. A **715**, 453 (2003); S.V. Afanasev, et al., NA49 Coll., Phys. Lett. B **491**, 59 (2000); S.V. Afanasiev, et al., NA49 Coll., Phys. Lett. B **538**, 275 (2002).
- [27] C. Adler, et al., STAR Coll., Phys. Rev. Lett. **89**, 092301 (2002); J. Adams, et al., STAR Coll., Phys. Rev. Lett. **92**, 182301 (2004); J. Adams, et al., STAR Coll., Phys. Rev. C **70**, 041901 (2004); C. Adler, et al., STAR Coll., Phys. Lett. B **595**, 143 (2004); C. Adler, et al., STAR Coll., Phys. Rev. C **65**, 041901(R) (2002); C. Adler, et al., STAR Coll., Phys. Rev. C **66**, 061901(R) (2002); J. Adams, et al., STAR Coll., nucl-ex/0311017; J. Adams, et al., STAR Coll., Phys. Lett. B **567**, 167 (2003).
- [28] J. Sollfrank, J. Phys. G **23**, 1903 (1997).
- [29] J. Letessier, A. Tounsi, U. Heinz, J. Sollfrank J. Rafelski, Phys. Rev. Lett. **70**, 3530 (1993); C. Song, V. Koch, Phys. Lett. B **404**, 1 (1997).
- [30] A.S. Kapoyannis, C.N. Ktorides, A.D. Panagiotou, J. Phys. G **28**, L47 (2002).
- [31] Z. Fodor, S.D. Katz, K.K. Szabó, Phys. Lett. B **568**, 73 (2003).
- [32] N.G. Antoniou, F.K. Diakonou, A.S. Kapoyannis, Proc. 10th International Workshop on Multiparticle Production, Crete, Greece 8-15 June 2002. World Scientific, p.201;

N.G. Antoniou, A.S. Kapoyannis, Phys. Lett. B **563**, 165 (2003); N.G. Antoniou, F.K. Diakonou, A.S. Kapoyannis, Nucl. Phys. A **759**, 417 (2005).

Tables

$S + S$		$S + Ag$		$Pb + Pb$		$Au + Au$	
K^+	12.5 ± 0.4	K_s^0	15.5 ± 1.5	N_p	362 ± 5.1	Λ	17.20 ± 1.75
K^-	6.9 ± 0.4	Λ	15.2 ± 1.2	K^+	103 ± 7.1	$\bar{\Lambda}$	12.15 ± 1.25
K_s^0	10.5 ± 1.7	$\bar{\Lambda}$	2.6 ± 0.3	K^-	51.9 ± 3.6	Ξ^-	2.11 ± 0.23
Λ	9.4 ± 1.0	\bar{p}	2.0 ± 0.8	K_s^0	81 ± 4	Ξ^+	1.77 ± 0.19
$\bar{\Lambda}$	2.2 ± 0.4	$p - \bar{p}$	43 ± 3	ϕ	7.6 ± 1.1	$\Omega + \bar{\Omega}$	0.585 ± 0.150
\bar{p}	1.15 ± 0.40	$B - \bar{B}$	105 ± 12	Λ	53 ± 5	p	26.37 ± 2.60
$p - \bar{p}$	21.2 ± 1.3	$h^{(*)}$	186 ± 11	$\bar{\Lambda}$	4.64 ± 0.32	\bar{p}	18.72 ± 1.90
$B - \bar{B}$	54 ± 3			Ξ^-	4.45 ± 0.22	K_s^0	36.7 ± 5.5
$h^{(*)}$	98 ± 3			Ξ^+	0.83 ± 0.04	ϕ	5.73 ± 0.78
				Ω	0.62 ± 0.09	K^{*0}	10.0 ± 2.70
				$\bar{\Omega}$	0.20 ± 0.03	$\pi^{(*)}$	239 ± 10.6
				$\pi^{(*)}$	619 ± 35.4	$\pi^{(*)}$	239 ± 10.6
				$\pi^{(*)}$	639 ± 35.4	K^+/K^-	1.092 ± 0.023
						\bar{K}^{*0}/K^{*0}	0.92 ± 0.27
						$\bar{\Omega}/\Omega$	0.95 ± 0.16

(*) This multiplicity has not been used in the fits where the pions are excluded.

Table 1. The full phase space multiplicities from the collision experiments $S + S$ (NA35), $S + Ag$ (NA35) and $Pb + Pb$ (NA49), as well as the midrapidity multiplicities and ratios from $Au + Au$ (STAR), used in the fits.

(a) set A, Fit with all

	$S + S$	$S + Ag$	$Pb + Pb$	$Au + Au$
No pentaquarks				
χ^2/dof	6.04/3	4.18/1	17.51/7	13.62/9
$T \text{ (MeV)}$	204.2 ± 9.7	236 ± 19	193.4 ± 3.0	326 ± 76
λ_u	1.76 ± 0.15	1.77 ± 0.33	1.724 ± 0.097	1.20 ± 0.12
λ_d	1.339 ± 0.069	1.47 ± 0.19	1.640 ± 0.071	1.039 ± 0.014
λ_s	1.019 ± 0.023	1.020 ± 0.041	1.167 ± 0.013	1.0014 ± 0.0047
γ_u	0.567 ± 0.077	0.46 ± 0.14	0.448 ± 0.059	0.164 ± 0.091
γ_d	1.06 ± 0.14	0.70 ± 0.17	0.583 ± 0.053	0.606 ± 0.084
γ_s	0.517 ± 0.024	0.338 ± 0.043	0.378 ± 0.019	0.284 ± 0.069
VT^3	173 ± 43	350 ± 150	3671 ± 400	550 ± 180
$\mu_B \text{ (MeV)}$	234 ± 29	315 ± 80	297 ± 21	84 ± 38
With pentaquarks				
χ^2/dof	6.20/3	4.11/1	17.49/7	13.62/9
$T \text{ (MeV)}$	205 ± 10	235 ± 19	193.7 ± 3.0	326 ± 76
λ_u	1.76 ± 0.15	1.77 ± 0.33	1.724 ± 0.097	1.20 ± 0.12
λ_d	1.340 ± 0.070	1.46 ± 0.19	1.639 ± 0.071	1.039 ± 0.014
λ_s	1.022 ± 0.022	1.022 ± 0.040	1.168 ± 0.013	1.0015 ± 0.0047
γ_u	0.563 ± 0.075	0.46 ± 0.14	0.446 ± 0.059	0.164 ± 0.091
γ_d	1.05 ± 0.14	0.70 ± 0.16	0.582 ± 0.053	0.606 ± 0.084
γ_s	0.514 ± 0.017	0.340 ± 0.042	0.376 ± 0.019	0.284 ± 0.069
VT^3	173 ± 43	350 ± 150	3670 ± 400	550 ± 180
$\mu_B \text{ (MeV)}$	235 ± 30	313 ± 79	297 ± 21	84 ± 38

(b) set A, Fit with no π 's

	$S + S$	$S + Ag$	$Pb + Pb$	$Au + Au$
No pentaquarks				
χ^2/dof	0.36/2	0/0	8.97/5	1.83/8
$T(MeV)$	260 ± 23	259.3	174.3 ± 4.6	151.6 ± 3.4
λ_u	1.781 ± 0.082	1.6666	1.697 ± 0.060	1.0756 ± 0.0051
λ_d	1.514 ± 0.066	1.8180	1.710 ± 0.069	1.0729 ± 0.0055
λ_s	0.939 ± 0.013	0.9611	1.169 ± 0.012	1.0172 ± 0.0024
γ_u	0.548 ± 0.027	0.5819	0.670 ± 0.048	1.37 ± 0.14
γ_d	0.719 ± 0.061	0.5377	0.759 ± 0.055	1.75 (fixed)
γ_s	0.588 ± 0.022	0.4650	0.575 ± 0.063	1.93 ± 0.17
VT^3	67.3 ± 9.2	158.08	2426 ± 30	275 ± 23
$\mu_B(MeV)$	365 ± 41	442.4	279 ± 17	32.4 ± 1.9
With pentaquarks				
χ^2/dof	0.35/2	0/0	9.10/5	1.85/8
$T(MeV)$	258 ± 23	265.1	176.1 ± 5.0	151.8 ± 3.4
λ_u	1.773 ± 0.084	1.6664	1.700 ± 0.062	1.0761 ± 0.0052
λ_d	1.522 ± 0.080	1.8210	1.705 ± 0.069	1.0732 ± 0.0055
λ_s	0.943 ± 0.018	0.9612	1.170 ± 0.012	1.0178 ± 0.0025
γ_u	0.557 ± 0.071	0.5676	0.646 ± 0.055	1.36 ± 0.13
γ_d	0.72 ± 0.10	0.5237	0.741 ± 0.054	1.75 (fixed)
γ_s	0.597 ± 0.056	0.4544	0.555 ± 0.065	1.92 ± 0.17
VT^3	67 ± 14	153.42	2490 ± 85	274 ± 23
$\mu_B(MeV)$	365 ± 44	453.1	282 ± 18	32.6 ± 1.9

Table 2. The results of fits on the $S + S$ (NA35), $S + Ag$ (NA35), $Pb + Pb$ (NA49) and $Au + Au$ (STAR) data with the imposition of the set of constraints A, without and with the inclusion of the pentaquark states. In part (a) all the multiplicities have been included in the fit and in part b) the multiplicities that contain pions have been excluded from the fit. In part (b) the fit on the STAR data has been performed with the variable γ_d held fixed at the given value. Table 2 (a) or 2 (b) contains the extracted parameters which are concluded as the freeze-out conditions for the $Pb + Pb$ case.

(a) set B, Fit with all

	$S + S$	$S + Ag$	$Pb + Pb$	$Au + Au$
No pentaquarks				
χ^2/dof	14.76/5	5.77/3	162.13/9	42.50/11
T (MeV)	243 ± 26	275 ± 55	437 ± 32	345 ± 63
λ_u	1.536 ± 0.038	1.613 ± 0.046	1.668 ± 0.084	1.082 ± 0.021
λ_d	1.534 ± 0.038	1.638 ± 0.048	1.728 ± 0.095	1.086 ± 0.022
γ_u	0.58 ± 0.12	0.46 ± 0.14	0.273 ± 0.019	0.350 ± 0.065
γ_d	0.58 ± 0.12	0.47 ± 0.14	0.293 ± 0.021	0.381 ± 0.069
γ_s	0.401 ± 0.094	0.308 ± 0.095	0.188 ± 0.011	0.322 ± 0.061
VT^3	152.2 ± 9.5	280 ± 12	678 ± 77	378 ± 53
μ_B (MeV)	313 ± 36	403 ± 82	702 ± 74	84 ± 22
$V_0(10^{-11} MeV^{-4})$	5.4 ± 2.0	4.9 ± 1.4	2.33 ± 0.35	3.58 ± 0.62
$B^{1/4}$ (MeV)	325 ± 37	359 ± 74	548 ± 40	441 ± 83
With pentaquarks				
χ^2/dof	14.99/5	5.78/3	162.65/9	42.53/11
T (MeV)	246 ± 22	278 ± 74	439 ± 32	346 ± 63
λ_u	1.536 ± 0.038	1.613 ± 0.046	1.668 ± 0.084	1.082 ± 0.021
λ_d	1.535 ± 0.038	1.638 ± 0.048	1.728 ± 0.095	1.086 ± 0.022
γ_u	0.58 ± 0.10	0.45 ± 0.18	0.272 ± 0.019	0.349 ± 0.064
γ_d	0.58 ± 0.10	0.47 ± 0.19	0.293 ± 0.021	0.380 ± 0.069
γ_s	0.397 ± 0.079	0.31 ± 0.13	0.188 ± 0.011	0.322 ± 0.061
VT^3	149.1 ± 8.5	274 ± 11	672 ± 76	377 ± 52
μ_B (MeV)	317 ± 32	407 ± 110	705 ± 74	85 ± 22
$V_0(10^{-11} MeV^{-4})$	5.5 ± 1.5	4.9 ± 1.6	2.31 ± 0.35	3.57 ± 0.63
$B^{1/4}$ (MeV)	328 ± 31	362 ± 100	551 ± 41	442 ± 82

(b) set B, Fit with no π 's

	$S + S$	$S + Ag$	$Pb + Pb$	$Au + Au$
No pentaquarks				
χ^2/dof	1.88/4	0.13/2	127.72/7	10.72/9
T (MeV)	194.9 ± 4.4	209.3 ± 4.9	444 ± 38	218 ± 26
λ_u	1.605 ± 0.025	1.661 ± 0.011	1.746 ± 0.073	1.075 ± 0.012
λ_d	1.599 ± 0.025	1.695 ± 0.012	1.817 ± 0.083	1.080 ± 0.012
γ_u	0.949 ± 0.065	0.775 ± 0.048	0.261 ± 0.018	0.71 ± 0.21
γ_d	0.958 ± 0.067	0.793 ± 0.048	0.280 ± 0.020	0.76 ± 0.22
γ_s	0.847 ± 0.071	0.601 ± 0.042	0.199 ± 0.012	0.81 ± 0.27
VT^3	94.1 ± 6.5	199 ± 10	621 ± 67	269 ± 59
μ_B (MeV)	275.3 ± 9.3	327.0 ± 8.4	778 ± 79	49.5 ± 8.1
$V_0(10^{-11} MeV^{-4})$	6.8 ± 1.0	6.2 ± 0.8	2.2 ± 0.4	5.4 ± 4.6
$B^{1/4}$ (MeV)	278.9 ± 7.3	290.7 ± 7.6	557 ± 48	301 ± 41
With pentaquarks				
χ^2/dof	1.55/4	0.13/2	128.04/7	10.80/9
T (MeV)	196.7 ± 4.6	216.3 ± 5.2	446 ± 38	221 ± 26
λ_u	1.608 ± 0.023	1.663 ± 0.011	1.746 ± 0.073	1.075 ± 0.012
λ_d	1.603 ± 0.023	1.694 ± 0.012	1.817 ± 0.083	1.081 ± 0.012
γ_u	0.948 ± 0.069	0.726 ± 0.044	0.261 ± 0.018	0.69 ± 0.20
γ_d	0.956 ± 0.070	0.746 ± 0.045	0.280 ± 0.020	0.74 ± 0.21
γ_s	0.865 ± 0.078	0.562 ± 0.039	0.198 ± 0.012	0.79 ± 0.25
VT^3	88.5 ± 6.9	200 ± 10	615 ± 66	272 ± 58
μ_B (MeV)	279.1 ± 9.1	338.2 ± 8.7	781 ± 80	50.4 ± 8.2
$V_0(10^{-11} MeV^{-4})$	7.2 ± 0.9	6.3 ± 0.7	2.2 ± 0.4	5.4 ± 4.3
$B^{1/4}$ (MeV)	282.1 ± 7.5	298.4 ± 7.8	560 ± 48	305 ± 40

Table 3. The results of fits on the $S + S$ (NA35), $S + Ag$ (NA35), $Pb + Pb$ (NA49) and $Au + Au$ (STAR) data with the imposition of the set of constraints B, without and with the inclusion of the pentaquark states. In part (a) all the multiplicities have been included in the fit and in part (b) the multiplicities that contain pions have been excluded from the fit. Table 3 (b) contains the extracted parameters which are concluded as the freeze-out conditions for the $S + S$, $S + Ag$ and $Au + Au$ cases.

Figure Captions

Fig. 1 Temperature as a function of the baryon chemical potential at the QGP-Hadron gas transition line for $B^{1/4} = 280$ MeV, without (lines (a),(c)) and with (line (b)) the inclusion of the pentaquark states. Lines (a) and (b) are calculated with $V_0 = 1.4/(4B)$ and line (c) with $V_0 = 1.29/(4B)$. Line (d) is the phase transition curve calculated from lattice QCD in [21].

Fig. 2 Relative chemical equilibrium variable of u -quark, γ_u , as a function of the baryon chemical potential at the QGP-Hadron gas transition line. Lines (a)-(c) correspond to lines (a)-(c) of Fig. 1.

Fig. 3 Relative chemical equilibrium variable of d -quark, γ_d , as a function of relative chemical equilibrium variable of u -quark, γ_u , at the QGP-Hadron gas transition line for the isospin symmetric case. Lines (a)-(c) correspond to lines (a)-(c) of Fig. 1. The line $\gamma_d = \gamma_u$ is also depicted.

Fig. 4 Relative chemical equilibrium variable of s -quark, γ_s , as a function of the baryon chemical potential at the QGP-Hadron gas transition line. Lines (a)-(c) correspond to lines (a)-(c) of Fig. 1.

Fig. 5 Volume expansion ratio $x = V_{HG}/V_{QGP}$ between pure hadron and pure QGP phase at the same transition point, as a function of the baryon chemical potential, which was used in calculations in Figs. 1-4. Lines (a)-(c) correspond to lines (a)-(c) of Fig. 1. In lines (a) and (b) $x_1 = 1.1$ at $\lambda_{u1} = 14.2$ and $\epsilon = 1.5$ and in line (c) $x_1 = 1.12$ at $\lambda_{u1} = 14.2$ and $\epsilon = 1.15$.

Fig. 1

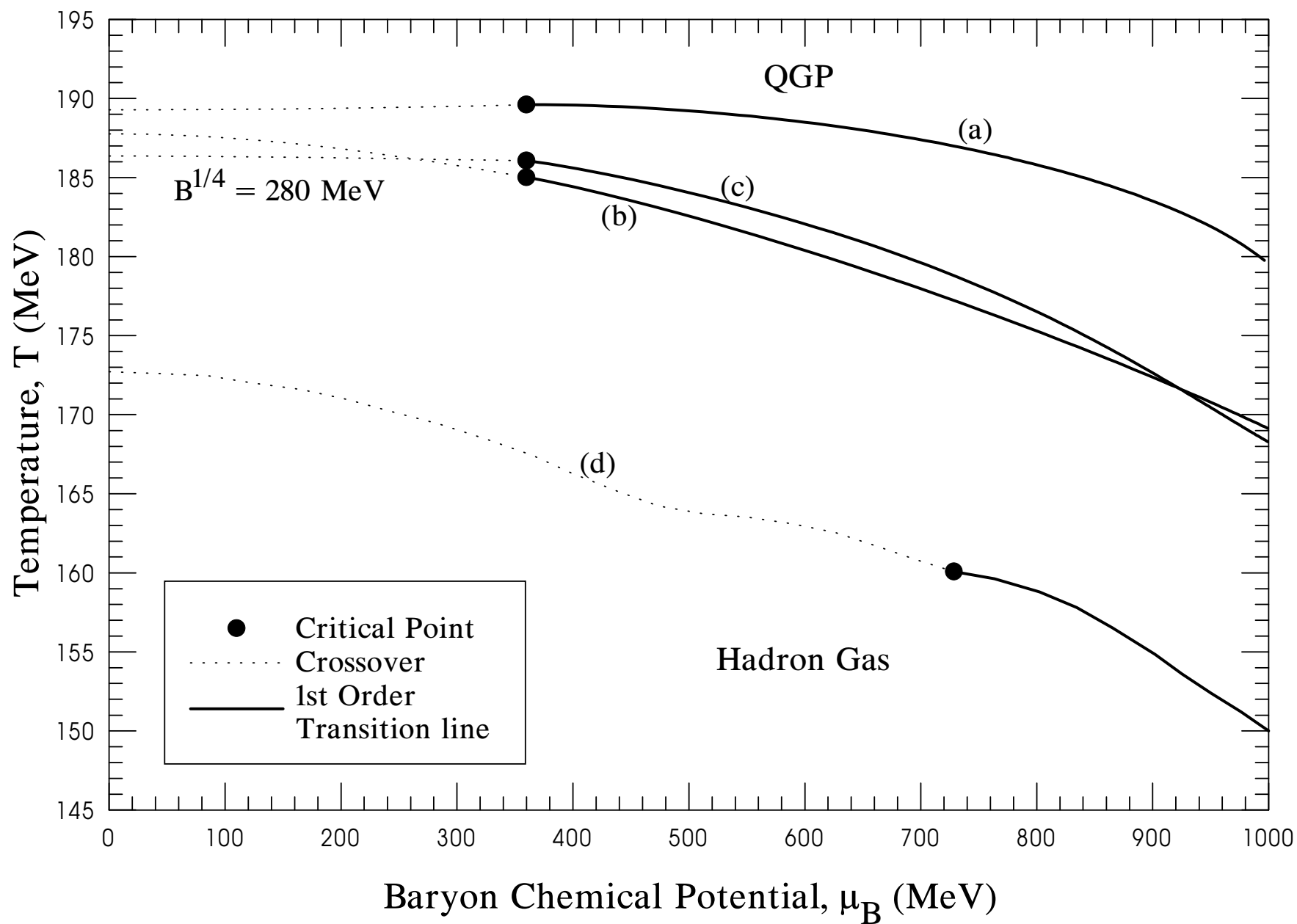


Fig. 2

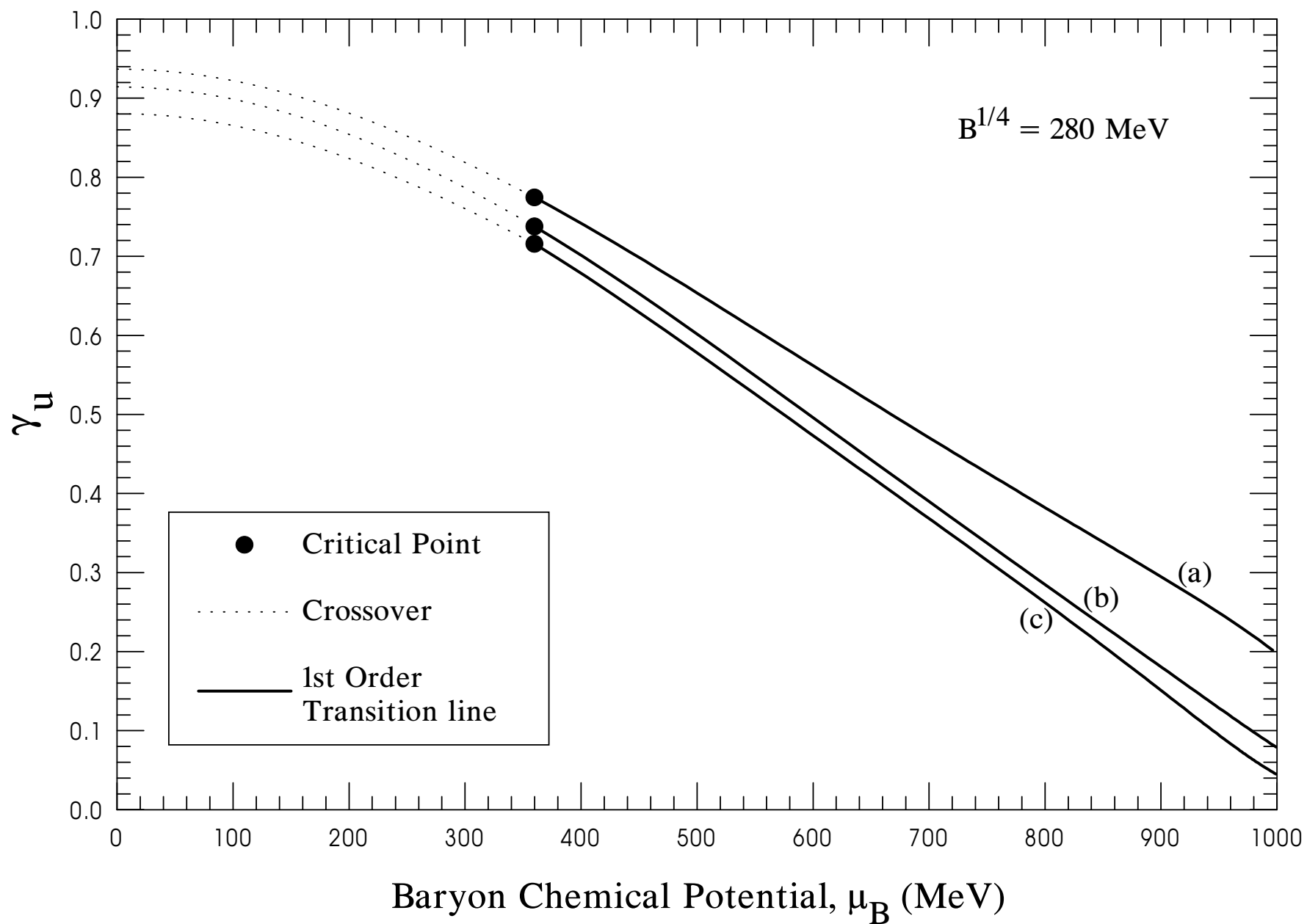


Fig. 3

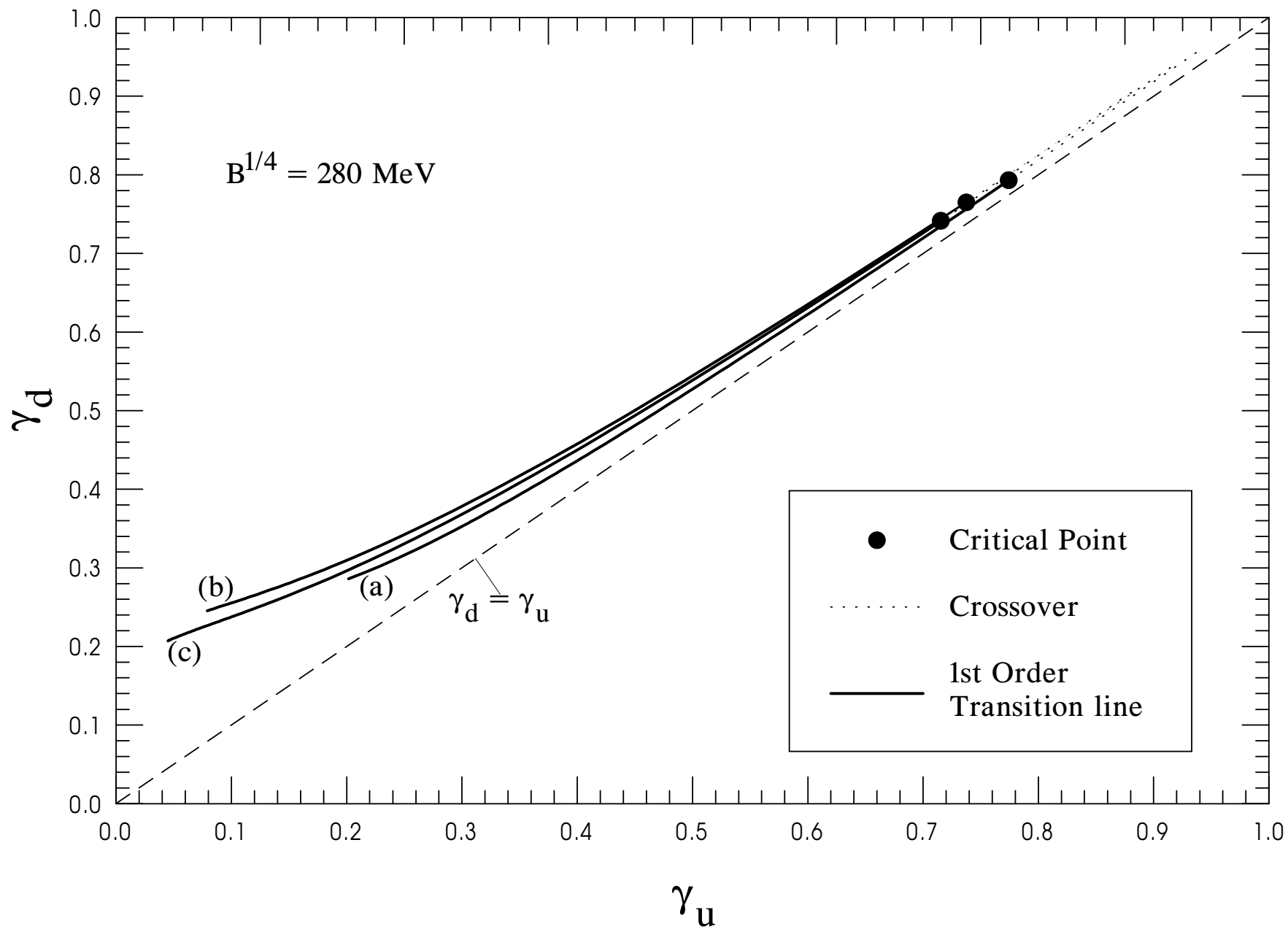


Fig. 4

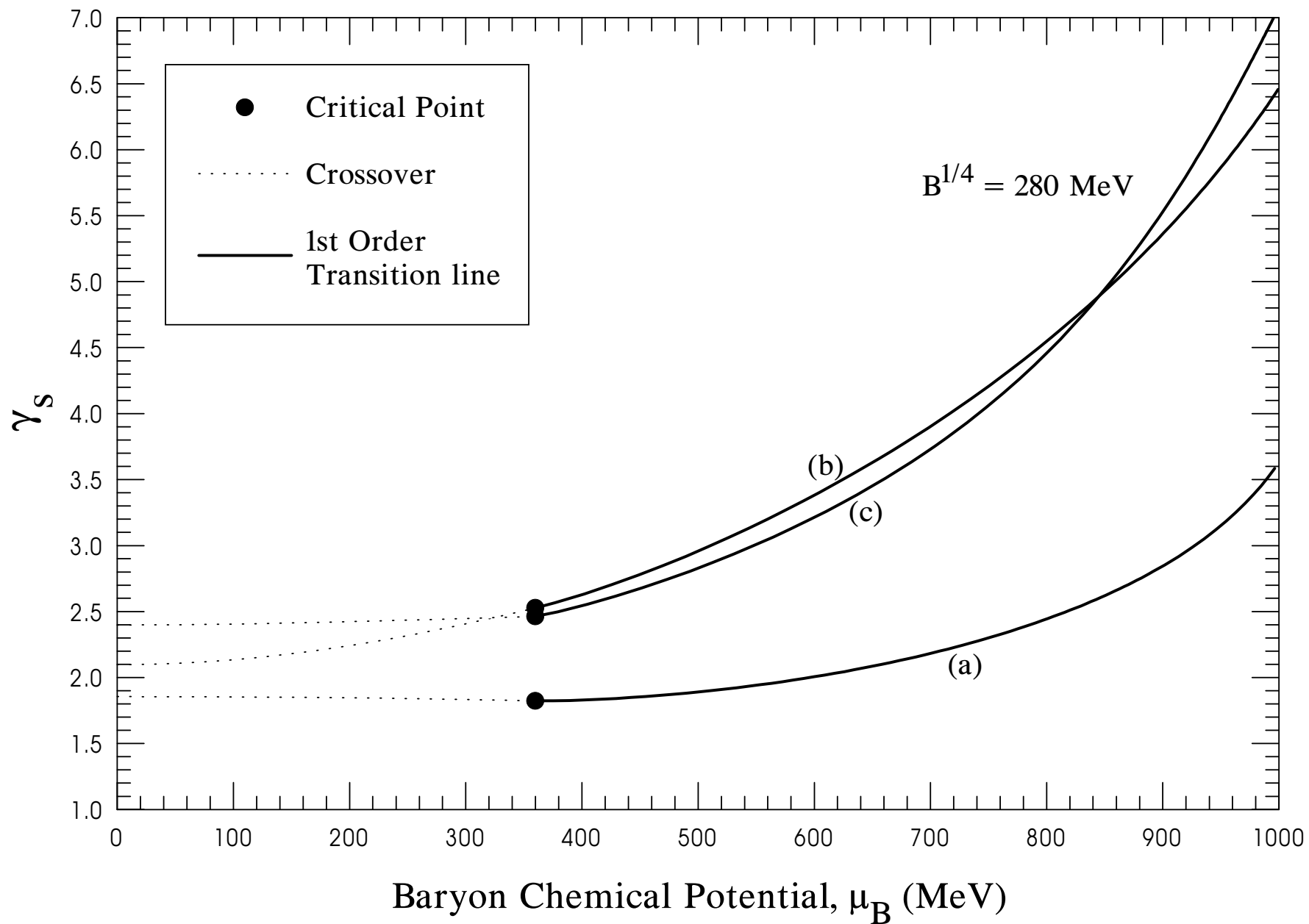


Fig. 5

